JOURNAL OF APPLIED ELECTROCHEMISTRY 20 (1990) 390–394

Limiting current in a high-temperature hydrogen pump with a $SrCeO_3$-based proton conductor

H. UCHIDA*, H. KIMURA, H. IWAHARA‡

Department of Environmental Chemistry and Technology, Faculty of Engineering, Tottori University, Koyama-cho, Tottori 680, Japan

Received 7 April 1989; revised 14 June 1989

Using a $SrCeO_3$-based proton conducting ceramic as a solid electrolyte, a high temperature hydrogen pump was constructed and the performance was examined at 650–800° C. The limiting diffusion current was measured as a function of hydrogen partial pressure at the anode by a potential sweep method with an automatic iR-compensation system. The limiting current density was a good measure of stable operating conditions for the hydrogen pump.

1. Introduction

The oxygen pump with solid oxide electrolyte has been widely used to control oxygen partial pressure. Recently, this device was noted as an interesting reactor for oxidation and reduction of organic or inorganic gases [1–9]. If one can use a high temperature proton conductor as a solid electrolyte, an electrochemical hydrogen extractor (hydrogen pump) can be constructed. Figure 1 shows the principle of operation of a hydrogen pump. Protons formed at the anode are forced to migrate toward the cathode by the electric field and discharge to generate hydrogen at the cathode. Thus, this electrochemical cell is useful for extracting pure hydrogen from gaseous mixtures and may also be applied in hydrogenation or dehydrogenation of various gases.

One of the candidates for the solid electrolyte in such a cell is $SrCe_{0.5}Yb_{0.05}O_{3-\alpha}$, which was found to be a good proton conducting ceramic [10]. We have already reported that the hydrogen pump could be constructed with this ceramic electrolyte at high temperature [11–17]. In this cell, hydrogen was extracted from the pyrolyzed gas of a $CO + H_2O$ mixture, ethane, methanol vapour and steam. However, since the current efficiency for hydrogen extraction decreased at high current density, it is necessary to determine the stable operating domain for efficient hydrogen pumping.

In this study, using a Yb-doped $SrCeO_3$ proton conducting solid electrolyte, a high temperature hydrogen pump was constructed and the performance was examined at 650–800° C. The limiting diffusion current was measured as a function of hydrogen partial pressure at the anode by a potential sweep method with automatic iR-compensation. The limiting current density was a good measure of stable operating conditions for the hydrogen pump.

2. Experimental details

The solid proton conductor used in this experiment was $SrCe_{0.95}Yb_{0.05}O_{3-\alpha}$, where α is the number of oxygen deficiencies per perovskite type unit cell. The construction of the solid electrolyte hydrogen pump was the same as in [11, 12]. The dense ceramic disc (thickness, about 0.5 mm; diameter, 12 mm) was used as the electrolyte diaphragm. Porous platinum electrodes were attached to both faces of the electrolyte disc (projected area, 0.5 cm^2). The electrode compartments were separated by the ceramic electrolyte and each compartment was sealed by a glass ring gasket.

A platinum wire was wound around the side of the disc as the reference electrode (R.E.). The R.E. may act as a hydrogen electrode, the potential of which depends on the partial pressure of hydrogen produced by the thermal dissociation equilibrium between water vapour and oxygen in the atmosphere at elevated temperature. Therefore, this electrode exhibited a different potential depending on the cell temperature and the humidity of the air. All the electrode potentials are referred to this electrode (R.E.) in this paper.

Pure hydrogen and a gaseous mixture of hydrogen and argon were supplied to each compartment at 1 atm (1.013×10^5 Pa) in the wet state ($P_{H_2O} \sim$ 20 torr). The gas flow rate was 60–100 ml min^{-1}. The hydrogen concentration in the gas was analysed by gas chromatography (Shimazu, Model GC-3BT; carrier gas, argon; column packing, molecular sieve 5A). In the polarization measurements, to determine the limiting current, hydrogen was extracted from the gas mixture (H_2 + Ar) to the pure hydrogen compartment.

Although a steady-state polarization method may be desirable to determine the limiting current, this may damage the electrolyte especially at high current over a long term operation. As a simple, rapid and direct measurement, we used a potential sweep

* Present address: Department of Applied Chemistry, Faculty of Engineering, Osaka University, Yamada-oka, Suita, Osaka 565, Japan.
‡ Present address: Synthetic Crystal Research Laboratory, Faculty of Engineering, Nagoya University, Furo-cho, Chikusa-ku, Nagoya 464, Japan.

0021-891X/90 $03.00 + .12

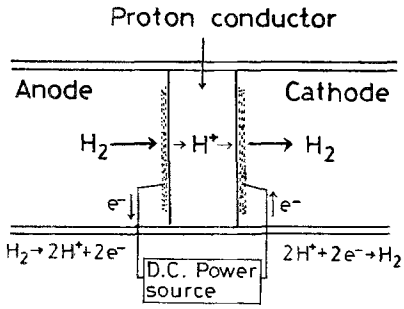

Fig. 1. Concept of hydrogen pump with solid proton conducting electrolyte.

method. Figure 2 shows the schematic diagram for the measuring instruments. This system consisted of normal potential-sweep units and instruments for non-feedback type iR-compensation. We employed a potentiostat (Nikko Keisoku, NPGS-301), a potential sweeper (Hokuto Denko, HB-103), an oscillator (NF Circuit Block, FG-121B), an auto-phase lock-in amplifier (NF Circuit Block, LI-574) and a personal computer (NEC, PC-8801 MkII SR) for data processing.

The polarization measurements were carried out as follows. Using a summing amplifier, a sine wave with a constant amplitude, $V_{a.c.}$ (0.1–2 mV), from an oscillator was superimposed on the signal for the potential sweep. When the potential E was scanned against the reference electrode, the cell current consisted of two components, a d.c. component (pumping current, i_{pump}) and an a.c. component $i_{a.c.}$. From $i_{a.c.}$ and $V_{a.c.}$, we calculated the a.c. impedance $R_{a.c.}$ of the electrolyte between the working and the reference electrode ($R_{a.c.} = V_{a.c.}/i_{a.c.}$). In order to measure $R_{a.c.}$ for the bulk ohmic resistance of the electrolyte, the frequency was usually set at 10 kHz, since the a.c. complex impedance of the cell converged to the real axis at around 10 kHz in the temperature range 600–800° C. Of the output current signals from the potentiostat, only the $i_{a.c.}$ with the same frequency as the reference signal was amplified by the lock-in amplifier. These signals (E, i_{pump}, $i_{a.c.}$) were treated with a personal computer

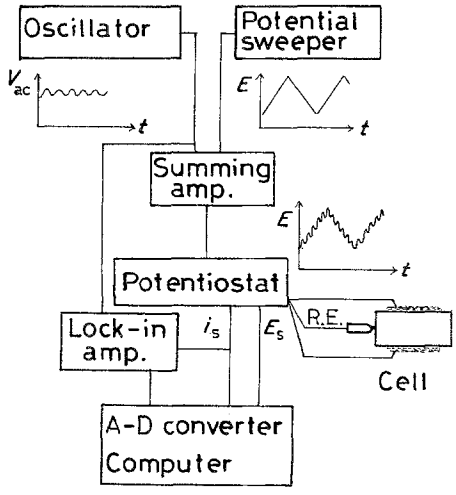

Fig. 2. Schematic diagram of experimental apparatus for potential sweep with iR-compensation: E_s, potential; i_s, current (converted to voltage signal by potentiostat).

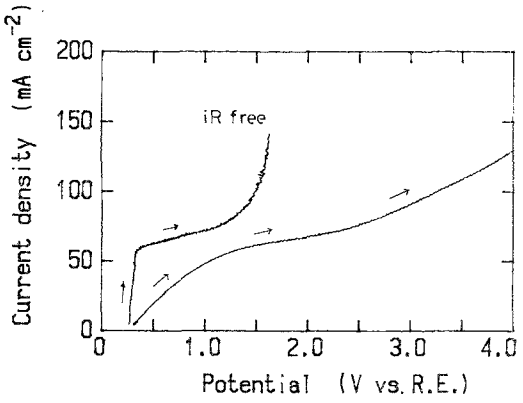

Fig. 3. Anodic polarization curves with and without iR-compensation on single potential sweep for the hydrogen pump at 750° C: Potential sweep rate, 50 mV s^{-1}; Electrolyte, $SrCe_{0.95}Yb_{0.05}O_{3-\alpha}$; Anode gas, H_2 + Ar ($P_{H_2} = 6.9 \times 10^{-3}$ atm); Cathode gas, H_2 (1 atm).

through 12 bit A–D converter (NEOLOG, PCN-1211). The E–i curves with and without iR-compensation and the E–$R_{a.c.}$ curve were drawn by using an X–Y plotter (Roland, DXY-880).

3. Results and discussion

3.1. *Polarization curve for hydrogen pump*

When pure hydrogen and the gas (Ar + H_2) mixture were introduced to the cell with $SrCe_{0.95}Yb_{0.05}O_{3-\alpha}$ ceramic electrolyte, the cell gave rise to a stable e.m.f., the electrode with higher P_{H_2} being the negative electrode. Since the e.m.f. of the hydrogen concentration cell was close to the theoretical limit, the proton transport number in this ceramic was close to unity under hydrogen atmosphere [10–18].

Figure 3 shows typical anodic polarization curves on potential sweep in the hydrogen pump, which extracts hydrogen from Ar + H_2 into the pure hydrogen compartment. In order to measure a polarization curve as rapidly as possible and to find a distinct limiting current density i_{lim}, various sweep rates were examined. The most suitable sweep rate was 50 mV s^{-1}. A single sweep was carried out from the rest potential toward positive potential (3–4 V). Because of the relatively large ohmic loss, the current varied gradually

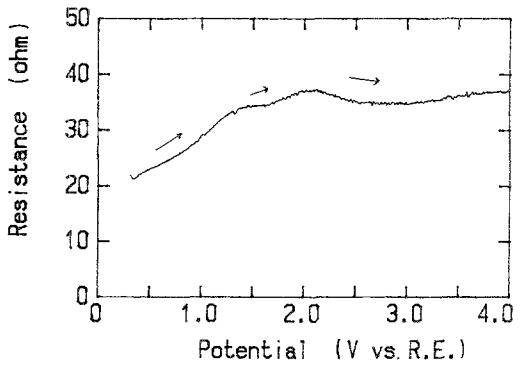

Fig. 4. Change in the impedance of the anode side in the electrolyte on single potential sweep. Conditions are same as in Fig. 3. (Potential contains iR loss.)

with the potential, although a shoulder-like limiting current was observed at 1.5–2 V with respect to R.E.

When the ohmic loss was excluded, the profile of the *i–E* curve became more definite as shown in Fig. 3. The shape of the polarization curve (iR free) was analogous to that observed in a zirconia cell under cathodic polarization [19, 20]. With increasing potential, the pumping current increases smoothly near the rest potential and reached a limiting current. After the saturation region, the current increased again probably because of partial electronic conduction, as described later.

The change in $R_{a.c.}$ on potential sweep is shown in Fig. 4. The impedance of the anode side of the electrolyte increased with increasing potential. On the other hand, at this time, a decrease in the impedance was observed at the cathode side of the electrolyte. When the potential was readjusted to the rest potential, each impedance returned to its original value. These results may be explained as follows. The proton conductivity σ_H varies with proton concentration $[H^+]$ in the electrolyte, since $\sigma_H = [H^+]e\mu_H$, where e and μ_H are the elementary charge and the mobility of the proton, respectively. Therefore, the change in impedance may be ascribed to a non-uniform distribution of protons in the oxide under the influence of the applied electric field. Since the source of protons (hydrogen) was limited by diffusion, the applied potential may cause a depletion of protons near the anode (increase in the impedance). On the cathode side, an increase in $[H^+]$ may give a $\Delta R_{a.c.}$ of opposite sign. As shown in Fig. 4, at high applied potential over 2 V, the impedance may be decreased by partial electronic conduction.

Figure 5 shows polarization curves (iR free) under various hydrogen partial pressures, P_{H_2}, at 800° C. A reversible behaviour of the pumping current was observed near the rest potential in all cases. The limiting current increased with increasing P_{H_2}.

3.2. *Dependence of limiting current on P_{H_2} and temperature*

The limiting current density was plotted against P_{H_2} at 650–800° C in Fig. 6. When the limiting value was not clear in the high P_{H_2} region, we determined a critical value from the inflection point of the smoothed *i–E* curve. A fairly good linear relationship was observed between log i_{lim} and log P_{H_2} at each temperature. The slope of each line was close to unity

$$i_{lim} \propto P_{H_2}. \quad (1)$$

This indicates that the limiting current density is controlled by diffusion of molecular hydrogen rather than by hydrogen atoms.

Figure 7 is a plot of E as a function of log $[i/(i_{lim} - i)]$ [19]. If i_{lim} is a diffusion controlled current and the charge transfer is reversible, the following equation should be valid

$$E = E_{1/2} + (RT/nF) \ln [i/(i_{lim} - i)] \quad (2)$$

where $E_{1/2}$ is the half-wave potential. In Equation 2, n should be two when the diffusing species is the hydrogen molecule. The results in Fig. 7 almost satisfy Equation 2 with $n = 2$, except at low current and near the i_{lim} region, where errors are large in the calculation. Hence, the iR-compensation was correctly made by this method. From Figs 6 and 7, it was confirmed that the limiting current density controlled by diffusion of molecular hydrogen could be determined by the potential sweep method with automatic iR-compensation in the hydrogen pump.

Figure 8 shows Arrehnius plots of i_{lim} at constant P_{H_2}. The limiting current density, i_{lim}, increased with

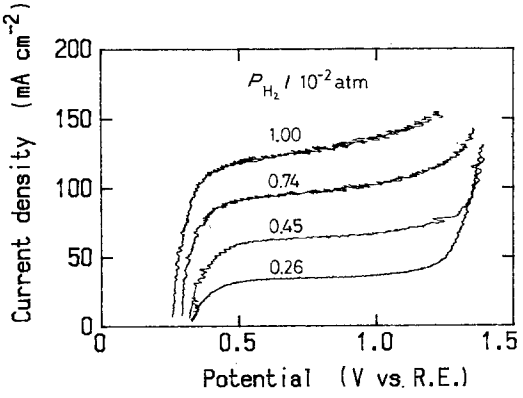

Fig. 5. Anodic polarization curve (iR free) for the hydrogen pump at 800° C under various P_{H_2}: Sweep rate, 50 mV s^{-1}; Anode gas, H_2 + Ar (P_{H_2} is shown on each curve); Cathode gas, H_2 (1 atm).

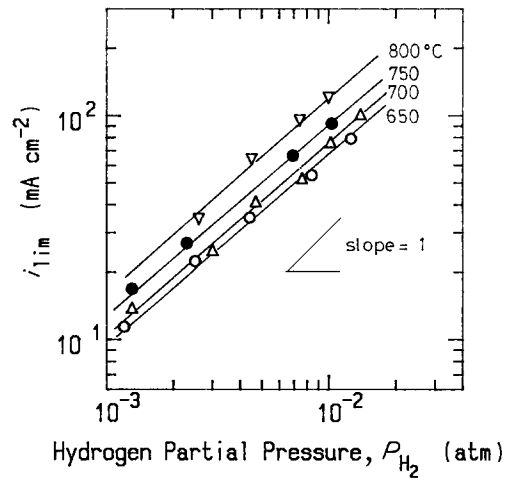

Fig. 6. Plots of log i_{lim} against log P_{H_2} in the hydrogen pump.

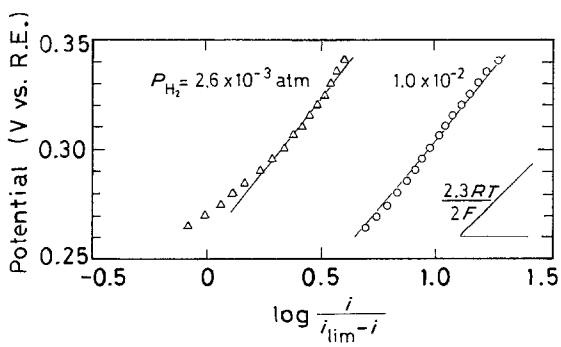

Fig. 7. Plots of E against log $[i/(i_{lim} - i)]$ at 800° C.

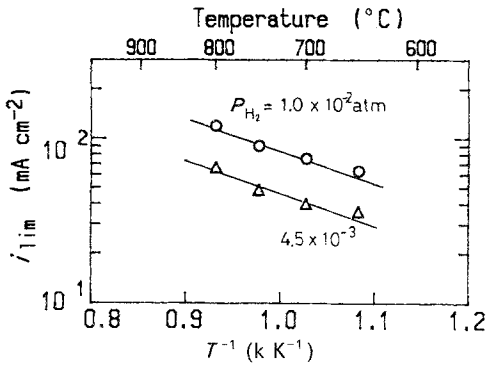

Fig. 8. Arrhenius plot of i_{lim} against T^{-1}.

temperature and the activation energy was about 0.5 eV. At 800° C, the i_{lim} exceeded 100 mA cm^{-2} at P_{H_2} = 0.01 atm. Such relativley large i_{lim} is reasonable because the anodic polarization in the fuel cell using this electrolyte above 800° C was very small at high P_{H_2} [11, 12, 14, 17, 21].

It is difficult to compare the limiting current densities with those reported in other solid electrolyte systems since i_{lim} depends on the morphology of the electrode. However, i_{lim} in this hydrogen pump seemed to be higher than those for oxygen pumping [19, 20, 22, 23] and the activation energy was relatively small.

3.3. *Change in current efficiency for hydrogen pumping*

Under various current density conditions we examined the current efficiency, ε(%), for hydrogen pumping

$$\varepsilon = uC/r_{theo} \quad (3)$$

where u and C are the gas flow rate and the hydrogen concentration (%) at the outlet of the cathode compartment, respectively. The theoretical evolution rate, r_{theo}, in Equation 3 was calculated from Faraday's law. Hydrogen was extracted from diluted hydrogen (3.3 × 10^{-3} atm) into the cathode. In order to carry the evolved hydrogen to a gas chromatograph, dry argon gas was passed through the cathode compartment at a constant flow rate. Before hydrogen extraction, the limiting current for the cell was measured in the manner described above. The limiting current density was about 40 mA cm^{-2} at 700° C as shown in Fig. 9a. Then, the hydrogen pump was operated at 30–100 mA cm^{-2} and the hydrogen evolution rate was measured at the cathode.

Below the limiting current density (30 mA cm^{-2}), the current efficiency was greater than 95% and was stable with time. In our previous work, a similar high efficiency was obtained in the hydrogen extraction from various gases [12–15, 17], since the hydrogen concentration was relatively high and the current density sufficiently low.

When the current was increased above i_{lim}, a decrease in the current efficiency was observed due to a partial electronic conduction as well as protonic conduction. We have reported that the electronic conductivity in these ceramics is about two orders of magnitude lower

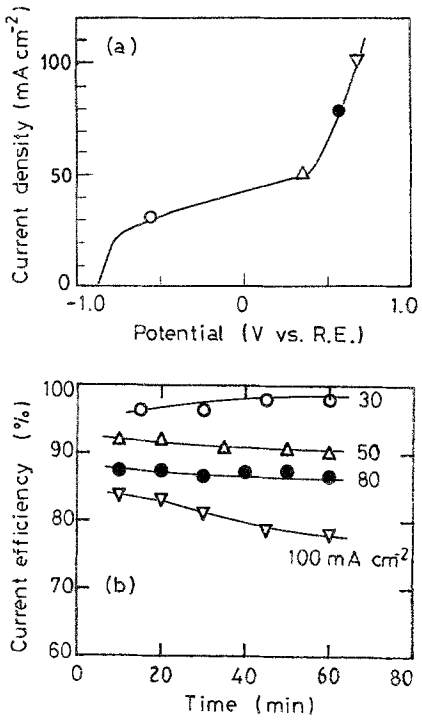

Fig. 9. Dependence of current efficiency on current density in the hydrogen pump at 700° C: Anode gas, H_2 + Ar (P_{H_2} = 3.3 × 10^{-3} atm); Cathode gas, dry Ar to carry evolved hydrogen. (a) Anodic polarization curve (iR free) before hydrogen-pumping. Sweep rate = 50 mV s^{-1}. (Symbols on the curve correspond to the current density operated in (b).) (b) Change in current efficiency for hydrogen-pumping with time.

than the protonic conduction in the hydrogen concentration cell [15]. However, under a high applied potential, additional electronic conduction may appear when the supply of hydrogen is limited by gas diffusion. At the extremely high current range (~ 100 mA cm^{-2}), the current efficiency decreased gradually with time. This means that operation with excess current may damage the protonic conduction mechanism in the electrolyte.

Consequently, the limiting current density determined by this method is a good measure of stable operating conditions for hydrogen pumping. Studies of a hydrogen pump with large electrode area for practical applications are in progress.

4. Conclusion

Using a Yb-doped $SrCeO_3$ proton conducting solid electrolyte, a high temperature hydrogen pump was constructed and the performance was examined at 650–800° C. The limiting diffusion current could be easily measured by a potential sweep method with an automatic iR-compensation system. The current efficiency for hydrogen pumping was stable above 95% below the limiting current density measured by this method. Therefore, this method is effective in evaluating the critical current density for stable steady operation of the hydrogen pump.

Acknowledgement

We thank the Ministry of Education, Science and

Culture of Japan for supporting part of this work by a Grant (63470061).

References

[1] S. Pancharatnam, R. A. Huggins and D. M. Mason, *J. Electrochem. Soc.* **122** (1975) 869.
[2] T. M. Gur and R. A. Huggins, *ibid.* **126** (1979) 1067.
[3] R. D. Farr and C. G. Vayenas, *ibid.* **127** (1980) 1478.
[4] T. M. Gur and R. A. Huggins, *Solid State Ionics* **5** (1981) 563.
[5] N. Stoukides and C. G. Vayenas, *J. Catal.* **70** (1981) 137.
[6] *Idem, J. Electrochem. Soc.* **131** (1984) 839.
[7] J. N. Michaels and C. G. Vayenas, *ibid.* **131** (1984) 2544.
[8] K. Otsuka, S. Yokoyama and A. Morikawa, *Bull. Chem. Soc. Jpn* **57** (1984) 3286.
[9] *Idem, Chem. Lett.* (1985) 319.
[10] H. Iwahara, T. Esaka, H. Uchida and N. Maeda, *Solid State Ionics* **3/4** (1981) 359.
[11] H. Iwahara, H. Uchida and N. Maeda, *J. Power Sources* **7** (1982) 293.
[12] H. Iwahara, H. Uchida and S. Tanaka, *Solid State Ionics* **9/10** (1983) 1026.
[13] H. Iwahara and H. Uchida, Proceedings of the International Meeting on Chemical Sensors (1983, Fukuoka, Japan) p. 227.
[14] H. Iwahara, H. Uchida and S. Tanaka, *J. Appl. Electrochem.* **16** (1986) 603.
[15] H. Iwahara, T. ESaka, H. Uchida, T. Yamauchi and K. Ogaki, *Solid State Ionics* **18/19** (1986) 1003.
[16] H. Iwahara, H. Uchida and I. Yamasaki, *Int. J. Hydrogen Energy* **12** (1987) 73.
[17] H. Iwahara, H. Uchida, K. Morimoto and S. Hosogi, *J. Appl. Electrochem.*, **19** (1989) 448.
[18] H. Iwahara, H. Uchida and N. Maeda, *Solid State Ionics* **11** (1983) 109.
[19] T. H. Etsell and S. N. Flengas, *J. Electrochem. Soc.* **118** (1971) 1890.
[20] T. M. Gur, I. D. Raistrick and R. A. Huggins, *ibid.* **127** (1980) 2620.
[21] H. Uchida, S. Tanaka and H. Iwahara, *J. Appl. Electrochem.* **15** (1985) 93.
[22] D. Y. Wang and A. S. Nowick, *J. Electrochem. Soc.* **128** (1981) 55.
[23] D. Braunstein, D. S. Tannhauser and I. Ries, *ibid.* **128** (1981) 82.